The fcc-bcc crystallographic orientation relationship in AlxCoCrFeNi high-entropy alloys

Rao, J. C.; Ocelik, V.; Vainchtein, D.; Tang, Z.; Liaw, P. K.; De Hosson, J. Th. M.

Published in:
Materials Letters

DOI:
10.1016/j.matlet.2016.04.086

Publication date:
2016

Materials Letters 176 (2016) 29–32

Contents lists available at ScienceDirect

Materials Letters

journal homepage: www.elsevier.com/locate/matlet

The *fcc-bcc* crystallographic orientation relationship in $Al_xCoCrFeNi$ high-entropy alloys

J.C. Rao [a,b,*], V. Ocelík [b], D. Vainchtein [b], Z. Tang [c], P.K. Liaw [c], J.Th.M. De Hosson [b,**]

[a] Institute for Advanced Ceramics, School of Materials Science and Engineering, Harbin Institute of Technology, Harbin 150001, PR China
[b] Department of Applied Physics, Zernike Institute for Advanced Materials, University of Groningen, Nijenborgh 4, 9747 AG Groningen, The Netherlands
[c] Department of Materials Science and Engineering, The University of Tennessee, Knoxville, TN 37996, USA

ARTICLE INFO

Article history:
Received 27 January 2016
Received in revised form
6 April 2016
Accepted 10 April 2016
Available online 11 April 2016

Keywords:
High-entropy alloy
HEA
TEM
Ordering
Orientation relationship

ABSTRACT

This paper concentrates on the crystallographic-orientation relationship between the various phases in the Al-Co-Cr-Fe-Ni high-entropy alloys. Two types of orientation relationships of *bcc* phases (some with ordered B2 structures) and *fcc* matrix were observed in $Al_{0.5}CoCrFeNi$ and $Al_{0.7}CoCrFeNi$ alloys at room temperature: $(1\ -1\ 0)_{bcc}//(200)_{fcc}$, $[001]_{bcc}//[001]_{fcc}$, (b) $(1\ -1\ 1)_{B2}//(2-2\ 0)_{fcc}$, $[011]_{B2}//[11\sqrt{2}]_{fcc}$.

In 1995 a new alloy-design concept was proposed by Yeh et al. [1–3] that was coined as high-entropy alloys (HEAs). Ever since HEAs have attracted considerable research, in which more than five major elements are combined with an atomic percentage (at%) in the range of 5–35. In comparison with conventional alloys, a number of interesting phenomena are observed, like high-entropy, sluggish-diffusion, lattice-distortion and so-called cocktail effects [4]. Many HEA systems have been reported to have several promising properties and exciting industrial applications [1,3,5–13], which require high strength, thermal stability, as well as wear and oxidation resistance, such as in tools, molds, dies, radiation resistance, and furnace parts. Resent research of HEAs addresses mechanical [14–18], anticorrosion [19,20], hydrogen storage [21], thermophysical [22], and magnetic [23,24] properties.

The high-entropy effect, the key property, originates from the significantly-higher configurational entropy in HEAs. Such high mixing entropy can favor the formation of disordered solid-solution states and suppress the formation of intermetallic compounds, which is of paramount importance in the application of these alloys [25]. Small atomic-size differences and near-zero values of the absolute enthalpy of mixing facilitate the formation of solid solutions for equiatomic alloys [26,27].

Rather than forming a complex microstructure, HEAs tend to form a simple solid-solution structure, such as face-centered cubic (*fcc*, A1),[1] body-centered cubic (*bcc*, A2), and hexagonal close-packed (*hcp*, A3) structure, or a mixture of them. It was pointed out that the multi-principal elements HEAs could easily form simple solid solutions or nano-precipitates during solidification due to the high mixing entropy and sluggish cooperative diffusion of substitutional solute atoms [25].

Singh et al. [28] have developed an algorithm to analyze uniquely the chemical short-ranged order (SRO) in an N-component solid-solution alloy, i.e., thermodynamically-induced ordering fluctuations. Within the density-functional theory, an electronic-structure-based thermodynamic theory was used to calculate SRO in homogeneously-disordered substitutional N-component alloys. Using the Gibbs (compositional) space, an analytic transform of the SRO eigenvectors was derived, providing a unique description of the high-temperature SRO in N-component alloys and the low-temperature long-ranged order. The electronic-based thermodynamic theory and the new general analysis was applied to ternaries (A1 Cu-Ni-Zn and A2 Nb-Al-Ti) for validation, and then to 5-component Al-Co-Cr-Fe-Ni HEAs. SRO was also investigated in

* Corresponding author at: Institute for Advanced Ceramics, School of Materials Science and Engineering, Harbin Institute of Technology, Harbin 150001, PR China.
** Corresponding author.
E-mail addresses: jcrao@hit.edu.cn (J.C. Rao), j.t.m.de.hosson@rug.nl (J.Th.M. De Hosson).

[1] A1, A2, A3, B2, $L1_2$ are the *Strukturbericht* Designations for crystal structures.

http://dx.doi.org/10.1016/j.matlet.2016.04.086
0167-577X/

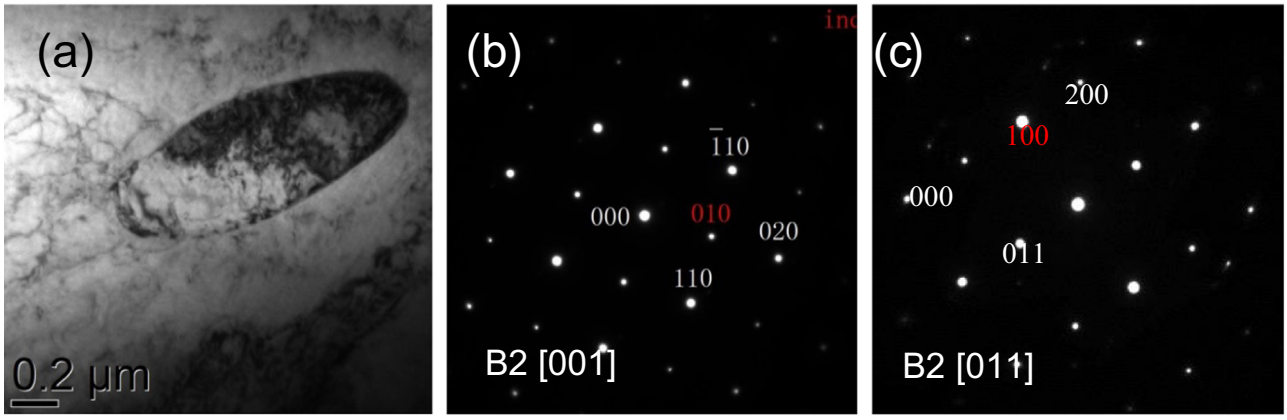

Fig. 1. TEM micrographs of the B2 phase in the $Al_xCoCrFeNi$ HEA at room temperature: (a) BF image showing the B2 phase (elliptical shape) embedded in the *fcc* matrix, (b, c) EDPs of the B2 phase in [001] and [011], respectively.

Table 1
EDS results of the B2 phase and *fcc* matrix in $Al_{0.5}CoCrFeNi$.

Phase	Constitution (atomic%)				
	Al	Co	Cr	Fe	Ni
fcc	7.20	20.09	23.14	25.07	24.51
B2	25.74	5.56	10.88	20.13	37.69

the Al-Co-Cr-Fe-Ni systems in three regions with different, aluminum contents, that is, poor with mole fraction $\Delta < 0.5$, aluminum intermediate with $0.5 \leq \Delta \leq 1.25$, and aluminum rich with $1.25 < \Delta \leq 2.0$, all of which show only simple solid-solution phases, i.e., A1, A2, or both. The thermodynamic predictions from the electronic-structure-based theories of the formation energy and short-range order from the linear response agree with experiments [28].

From this theoretical prediction, there exist no ordering structures in the Al-Co-Cr-Fe-Ni HEAs. However, instead of the homogeneous solid solution, nano-scaled phase separation takes place in the single-phase *fcc* HEAs. For example, the ordered *fcc* nanoparticle was discovered in the *fcc* matrix of $Al_{0.3}CoCrFeNi$ [25,29] and $Al_{0.5}CoCrCuFeNi$ [30]. It was reported that in the $Al_{0.3}CoCrFeNi$ alloy, the $L1_2$ ordered structure is a multi-elementally ordered solid solution instead of an intermetallic compound. This is because the high mixing entropy effect of multi-principal elements can effectively reduce the Gibbs free energy of mixing, and, consequently, forms a solid solution rather than an intermetallic compound during solidification. Meanwhile, the sluggish cooperative diffusion effect and the relatively-negative mixing enthalpies between Al and other compositional elements can effectively inhibit the phase growth and promote the nanoparticle formation [29].

Although there are a few publications on the ordered phases in HEAs, there is very scant information on the crystallographic-orientation relationship between the ordered phases and matrix. In the present study, the short-range ordering effects of the *bcc* phase in the *fcc* matrix in the $Al_{0.5}CoCrFeNi$ and $Al_{0.7}CoCrFeNi$ HEAs were studied on the morphology and the crystallographic-orientation relationship between the ordered phases and matrix.

Ingots with nominal compositions of $Al_{0.5}CoCrFeNi$ and $Al_{0.7}CoCrFeNi$ were prepared by arc-melting pure elements with purity higher than 99.95 wt% (wt%) under a high-purity argon atmosphere on a water-cooled Cu hearth. The alloys were re-melted four times in order to obtain homogeneity [31]. Next, they were homogenized at 1250 °C for 50 h after casting. Several thin foils for TEM (transmission electron microscopy) observation were prepared from the middle of the bulk materials by conventional mechanical grinding and polishing with SiC abrasive papers gradually and finished by ion milling at 4 kV in a PIPS 691 system (Gatan, Inc., Pleasanton, CA, USA). A JEM 2010F transmission electron microscope (JEOL Ltd., Tokyo, Japan), operating at 200 kV, equipped with an energy dispersive x-ray spectroscopy (EDS) system (127 eV resolution, Bruker Corporation, Billerica, MA, USA),

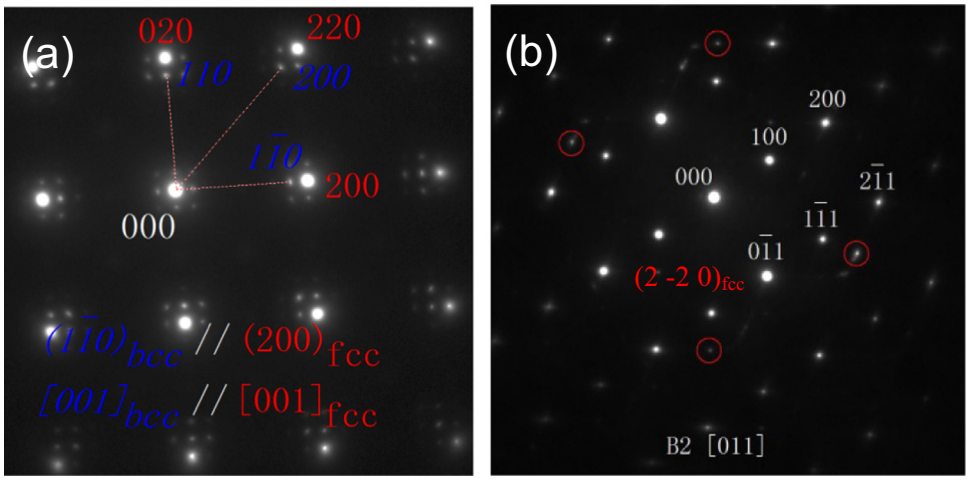

Fig. 2. EDPs showing two kinds of crystallographic-orientation relationships between the B2 phase and the *fcc* matrix in $Al_xCoCrFeNi$ at room temperature (a) $(1\ -1\ 0)_{bcc}$// $(200)_{fcc}$ and $[001]_{bcc}$//$[001]_{fcc}$ and (b) $(1\ -1\ 1)_{B2}$//$(2\ -2\ 0)_{fcc}$ and $[011]_{B2}$//$[11\sqrt{2}]_{fcc}$.

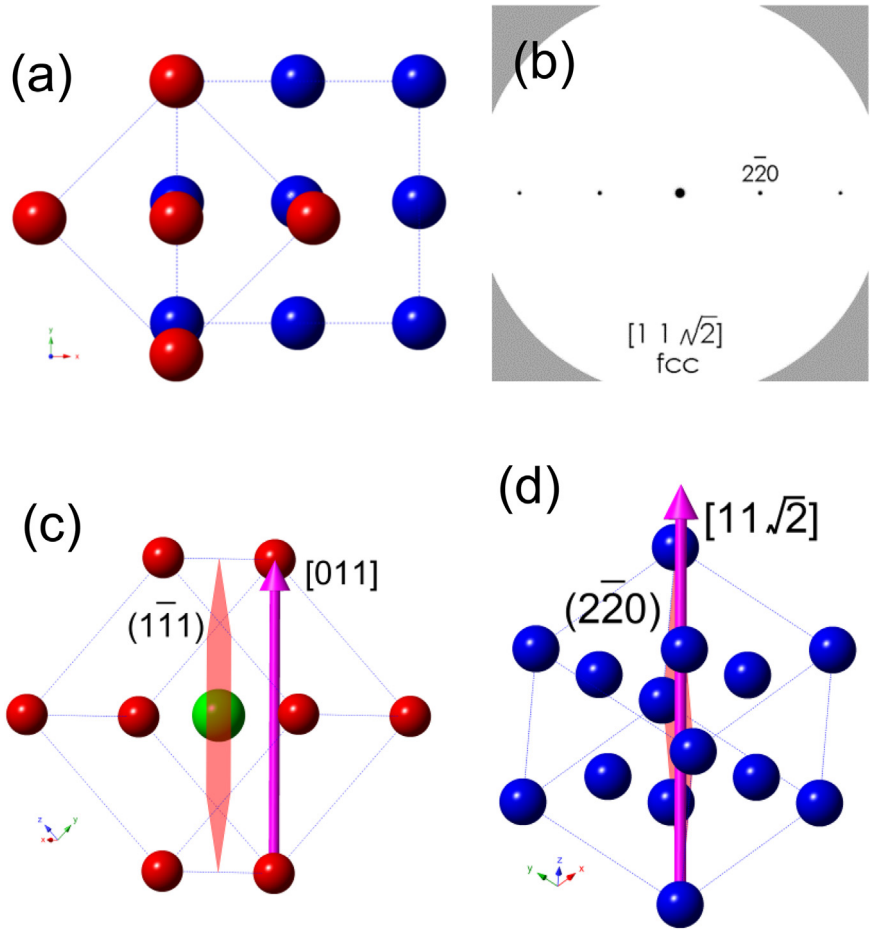

Fig. 3. Simulation results of the *bcc* and the B2 phases (red and green, respectively) with the *fcc* (blue) matrix in $Al_xCoCrFeNi$ HEAs. (a) unit-cell projection in the [001] direction showing $(1\ -1\ 0)_{bcc}//(200)_{fcc}$ and $[001]_{bcc}//[001]_{fcc}$. (b) simulated EDP of the *fcc* matrix in $[11\sqrt{2}]$, (c,d) $(1\ -1\ 1)_{B2}//(2\ -2\ 0)_{fcc}$ and $[011]_{B2}//[11\sqrt{2}]_{fcc}$. (For interpretation of the references to color in this figure legend, the reader is referred to the web version of this article.)

was used for the selected area-electron diffraction (SAED) and chemical composition analysis as well as TEM observations. Software CrystalMaker® (CrystalMaker Software Limited, Oxfordshire, UK) was used for the simulation of the unit cell structure and EDP (Please define EDP) of the studied phases.

The detailed TEM analysis confirmed that there are both *fcc* and *bcc* phases in the studied $Al_{0.5}CoCrFeNi$ and $Al_{0.7}CoCrFeNi$ alloys. The volume fraction of the *bcc* phase is less than that of the *fcc* matrix. The EDS results from different areas of the same grain with a 1-nm electron-beam size show that the material is homogeneous. The SAED patterns indicate that there are at least two sets of patterns for different phases instead of only one *fcc* phase in some area. Some *bcc* phase had transformed into the B2 ordered structure. Fig. 1(a) shows the bright-field (BF) image of a rugby-shaped grain embedded in the *fcc* matrix in $Al_{0.5}CoCrFeNi$ at room temperature. The EDPs are assigned to the B2 phase in [001] and [011] directions, as shown in Fig. 1(b) and (c), respectively. The nominal constitution in the atomic percentage of $Al_{0.5}CoCrFeNi$ is 11.1% for Al and 22.2% for the rest elements. However, the EDS results in Table 1 show that the B2 phase is rich in Al and Ni, with the lack of Cr and Fe. Meanwhile the adjacent *fcc* matrix is lack of Al. Based on these experimental results, we can reasonably infer that the B2 phase is a ordered NiAl intermetallic compound solidified with Co, Cr, and Fe inside, even these multi-elements mostly form the disordered solid solution, i.e., the *bcc* phase.

Whether we have a disordered *bcc* phase or ordered B2 phase, they form out of the *fcc* solid solution of $Al_{0.5}CoCrFeNi$ and $Al_{0.7}CoCrFeNi$. Therefore, there could be some relationship between them and the *fcc* matrix. Fig. 2 shows two kinds of crystallographic-orientation relationships between the *bcc* or B2 phase and *fcc* matrix in $Al_{0.5}CoCrFeNi$ at room temperature: (a) $(1\ -1\ 0)_{bcc}//(200)_{fcc}$, $[001]_{bcc}//[001]_{fcc}$ and (b) $(1\ -1\ 1)_{B2}//(2\ -2\ 0)_{fcc}$, $[011]_{B2}//[11\sqrt{2}]_{fcc}$. Fig. 2(b) is from the selected area across the interface between the B2 phase and the *fcc* matrix, while Fig. 1(c) is only from the B2 phase. It is clear by comparing these two figures that there are only four extra spots inside of the red circles of the *fcc* solid-solution matrix in Fig. 2(b), since the $[11\sqrt{2}]$ direction is a higher index zone axis. This trend will be illustrated in detail.

The structures of the *fcc* and the *bcc* as well as the B2 phases were put into the CrystalMaker software for simulation purposes. Fig. 3 gives the simulated results. The *bcc* and the B2 phase are shown with red (and green) balls, while the *fcc* matrix in blue. Fig. 3(a) is the unit cell projection in the [001] direction of the *bcc* phase and the *fcc* matrix together, showing clearly the orientation of $(1\text{-}1\ 0)_{bcc}//(200)_{fcc}$ and $[001]_{bcc}//[001]_{fcc}$. Fig. 3(b) gives the simulated EDP of the *fcc* matrix in the $[11\sqrt{2}]$ direction. Fig. 3(c,d) are the B2 phase in the [011] direction and the *fcc* matrix in the $[11\sqrt{2}]$ direction, respectively, showing the orientation relationship of $(1\ -1\ 1)_{B2}//(2\ -2\ 0)_{fcc}$ and $[011]_{B2}//[11\sqrt{2}]_{fcc}$.

It should be noted that nano-scaled *bcc* phase is also observed even in a lower Al content $Al_{0.3}CoCrFeNi$, which are homogeneously distributed in the *fcc* matrix with a basic crystallographic-orientation relationship between these two phases. The bcc phase is homogeneously distributed in all over the grain as well as the *fcc* phase, although some crystallites of the *fcc* phase

are coarsened. Finally, we conclude that special crystallographic-orientation relationships between the precipitates and matrix are discovered in more and more new multicomponent, including HEAs and other strengthening materials and detailed research on these aspects is necessary (see [32] and references therein) to reveal the structure-property relationship.

In summary, interestingly we found *two types* of orientation relationships of the *bcc* phases and the *fcc* matrix in $Al_{0.5}CoCrFeNi$ and $Al_{0.7}CoCrFeNi$ HEAs at room temperature. Some of the *bcc* phases are ordered ones into a B2 structure. These orientation relationships are described as follows: $(1\ -1\ 0)_{bcc}//(200)_{fcc}$ and $[001]_{bcc}//[001]_{fcc}$, (b) $(1\ -1\ 1)_{B2}//(2\ -2\ 0)_{fcc}$ and $[011]_{B2}//[11\sqrt{2}]_{fcc}$.

Acknowledgements

This work was supported by the Royal Netherlands Academy of Science (KNAW, Amsterdam) with Grant no. 11CDP003. J.C. Rao is grateful for the financial support of the National Natural Science Foundation of China (Grant no. 51572054, 51021002, and 51321061). J.C. Rao acknowledges the support of the Center of Analysis and Measurement of the Harbin Institute of Technology (CAM, HIT) for the short leave of absence. PKL would like to acknowledge the Department of Energy (DOE), Office of Fossil Energy, National Energy Technology Laboratory (DE-FE-0008855, DE-FE-0024054, and DE-FE-0011194), with Mr. V. Cedro, Mr. R. Dunst, and Dr. J. Mullen as program managers. PKL very much appreciate the support of the U.S. Army Research Office Project (W911NF-13-1-0438) with the program manager, Dr. D. M. Stepp. PKL thanks the support from the National Science Foundation (CMMI-1100080) with the program director, Dr. C. Cooper.

References

[1] J.W. Yeh, S.K. Chen, S.J. Lin, J.Y. Gan, T.S. Chin, T.T. Shun, C.H. Tsau, S.Y. Chang, Adv. Eng. Mater. 6 (2004) 299–303.
[2] M.H. Chuang, M.H. Tsai, W.R. Wang, S.J. Lin, J.W. Yeh, Acta Mater. 59 (2011) 6308–6317.
[3] Y. Zhang, T.T. Zuo, Z. Tang, M.C. Gao, K.A. Dahmen, P.K. Liaw, Z.P. Lu, Prog. Mater. Sci. 61 (2014) 1–93.
[4] J.W. Yeh, Ann. Chim. Sci. Mater. 31 (2006) 633–648.
[5] C.Y. Hsu, C.C. Juan, S.T. Chen, T.S. Sheu, J.W. Yeh, S.K. Chen, J. Miner. Mater. Met. Mater. Soc. 65 (2013) 1829–1839.
[6] C.Y. Hsu, J.W. Yeh, S.K. Chen, T.T. Shun, Metall. Mater. Trans. A 35 (2004) 1465–1469.
[7] J.W. Yeh, S.K. Chen, J.Y. Gan, S.J. Lin, T.S. Chin, T.T. Shun, C.H. Tsau, S.Y. Chang, Metall. Mater. Trans. A 35 (2004) 2533–2536.
[8] Y.Y. Chen, T. Duval, U.D. Hung, J.W. Yeh, H.C. Shih, Corros. Sci. 47 (2005) 2257–2279.
[9] C.J. Tong, M.R. Chen, S.K. Chen, J.W. Yeh, T.T. Shun, S.J. Lin, S.Y. Chang, Metall. Mater. Trans. A 36 (2005) 1263–1271.
[10] Y.J. Zhou, Y. Zhang, Y.L. Wang, G.L. Chen, Appl. Phys. Lett. 90 (2007) 181904.
[11] J.M. Zhu, H.F. Zhang, H.M. Fu, A.M. Wang, H. Li, Z.Q. Hu, J. Alloy. Compd. 497 (2010) 52–56.
[12] O.N. Senkov, G.B. Wilks, D.B. Miracle, C.P. Chuang, P.K. Liaw, Intermetallics 18 (2010) 1758–1765.
[13] L.J. Santodonato, Y. Zhang, M. Feygenson, C.M. Parish, M.C. Gao, R.J. Weber, J. C. Neuefeind, Z. Tang, P.K. Liaw, Nat. Commun. 6 (2015) 5964.
[14] Y.F. Kao, T.J. Chen, S.K. Chen, J.W. Yeh, J. Alloy. Compd. 488 (2009) 57–64.
[15] M.A. Hemphill, T. Yuan, G.Y. Wang, J.W. Yeh, C.W. Tsai, A. Chuang, P.K. Liaw, Acta Mater. 60 (2012) 5723–5734.
[16] Z. Tang, T. Yuan, C.W. Tsai, J.W. Yeh, C.D. Lundin, P.K. Liaw, Acta Mater. 99 (2015) 247–258.
[17] M. Seifi, D. Li, Z. Yong, P.K. Liaw, J. Lewandowski, J. Miner. Mater. Met. Mater. Soc. 67 (2015) 2288–2295.
[18] B. Gludovatz, A. Hohenwarter, D. Catoor, E.H. Chang, E.P. George, R.O. Ritchie, Science 345 (2014) 1153.
[19] Y.F. Kao, T.D. Lee, S.K. Chen, Y.S. Chang, Corros. Sci. 52 (2010) 1026–1034.
[20] Z. Tang, L. Huang, W. He, P.K. Liaw, Entropy 16 (2) (2014) 895–911.
[21] Y.F. Kao, S.K. Chen, J.H. Sheu, J.T. Lin, W.E. Lin, J.W. Yeh, S.J. Lin, T.H. Liou, C. W. Wang, Int. J. Hydrog. Energy 35 (2010) 9046–9059.
[22] H.P. Chou, Y.S. Chang, S.K. Chen, J.W. Yeh, Mater. Sci. Eng. B 163 (2009) 184–189.
[23] Y. Zhang, T.T. Zuo, Y.Q. Cheng, P.K. Liaw, Sci. Rep. 3 (2013) 1455.
[24] T.T. Zuo, X. Yang, P.K. Liaw, Y. Zhang, Intermetallics 67 (2015) 171–176.
[25] C.J. Tong, Y.L. Chen, S.K. Chen, J.W. Yeh, T.T. Shun, C.H. Tsau, S.J. Lin, S.Y. Chang, Metall. Mater. Trans. A 36 (2005) 881–893.
[26] Y. Zhang, Y.J. Zhou, J.P. Lin, G.L. Chen, P.K. Liaw, Adv. Eng. Mater. 10 (2008) 534–538.
[27] S. Singh, N. Wanderka, B.S. Murty, U. Glatzel, J. Banhart, Acta Mater. 59 (2011) 182–190.
[28] P. Singh, A.V. Smirnov, D.D. Johnson, Phys. Rev. B 91 (2015) 224204.
[29] T.T. Shun, C.H. Hung, C.F. Lee, J. Alloy. Compd. 493 (2010) 105–109.
[30] X.D. Xu, P. Liu, S. Guo, A. Hirata, T. Fujita, T.G. Nieh, C.T. Liu, M.W. Chen, Acta Mater. 84 (2015) 145–152.
[31] S.G. Ma, P.K. Liaw, M.C. Gao, J.W. Qiao, Z.H. Wang, Y. Zhang, J. Alloy. Compd. 604 (2014) 331–339.
[32] I. Konyashin, F. Lachmann, B. Ries, A.A. Mazilkin, B.B. Straumal, Chr Kuebel, L. Llanes, B. Baretzky, Scr. Mater. 83 (2014) 17–20.